



## Geomorphology of the northeastern extreme of Isla Grande de Tierra del Fuego, Argentina

Luis Díaz Balocchi , Juan Federico Ponce , Alfonsina Tripaldi & Ignacio Magneres


To cite this article: Luis Díaz Balocchi , Juan Federico Ponce , Alfonsina Tripaldi & Ignacio Magneres (2020) Geomorphology of the northeastern extreme of Isla Grande de Tierra del Fuego, Argentina, Journal of Maps, 16:2, 512-523, DOI: [10.1080/17445647.2020.1780168](https://doi.org/10.1080/17445647.2020.1780168)

To link to this article: <https://doi.org/10.1080/17445647.2020.1780168>



© 2020 The Author(s). Published by Informa UK Limited, trading as Taylor & Francis Group on behalf of Journal of Maps




[View supplementary material](#) 




Published online: 23 Jun 2020.



[Submit your article to this journal](#) 



[View related articles](#) 



[View Crossmark data](#) 



## Geomorphology of the northeastern extreme of Isla Grande de Tierra del Fuego, Argentina

Luis Díaz Balocchi<sup>a,b</sup>, Juan Federico Ponce<sup>a,c</sup>, Alfonsina Tripaldi<sup>b,d</sup> and Ignacio Magneres<sup>a</sup>

<sup>a</sup>Laboratorio de Geomorfología y Cuaternario, Centro Austral de Investigaciones Científicas (CADIC), CONICET, Ushuaia, Argentina; <sup>b</sup>Facultad de Ciencias Exactas y Naturales, Departamento de Ciencias Geológicas, Universidad de Buenos Aires, Buenos Aires, Argentina; <sup>c</sup>Instituto de Ciencias Polares, Ambiente y Recursos Naturales, Universidad Nacional de Tierra del Fuego, Ushuaia, Argentina; <sup>d</sup>Instituto de Geociencias Básicas, Aplicadas y Ambientales de Buenos Aires (IGEBA), CONICET – Universidad de Buenos Aires, Buenos Aires, Argentina

### ABSTRACT

A 1:60,000 scale geomorphological map of the Argentine side of the northeastern extreme of Isla Grande de Tierra del Fuego in southernmost South America is presented. This paper describes and summarizes the geomorphology of the mapped area, which includes glacial, periglacial, fluvial, coastal, aeolian, lacustrine, and anthropogenic landforms that span over 680 km<sup>2</sup> north of San Sebastián Bay in a sparsely populated semiarid and cold steppe used for sheep breeding and hydrocarbon extraction. We used Landsat-8, Sentinel-2, and ALOS-PALSAR satellite products combined with field validation to create the map. Glacial advances and retreats as well as climatic and sea level fluctuations that controlled fluvial systems and coastal dynamics were the main sculptors of the landscape during the Late Cenozoic. Aeolian, lacustrine, and anthropogenic activity were later minor contributors. The presented free, open access, vector geomorphological map is intended to be a supporting tool for multidisciplinary researchers and decision-makers.

### ARTICLE HISTORY

Received 20 September 2019  
Revised 14 May 2020  
Accepted 5 June 2020

### KEYWORDS

Magellan Strait; San Sebastián Bay; Patagonia; Late Cenozoic glaciations; hummocky moraine; glacial landsystems

## 1. Introduction

Isla Grande de Tierra del Fuego (IGTdf) is located at the southern extreme of South America (Main Map; Figure 1). It is enclosed by the southern Andes Range to the west and south, and surrounded by the Atlantic, Pacific, and Southern Oceans. IGTdf can be divided into two main morphological regions: the Fuegian Andes to the south and west, and the plains to the north (Fernández et al., 2018). During the Late Cenozoic, the landscape of IGTdf was intensely modified by several outlet glaciers that flowed down from the Cordillera Darwin ice sheet located in the Fuegian Andes (Caldenius, 1932; Nordenskjöld, 1899). At various times, glacial advances extended farther north and east than the mountain range, into the plains, reaching the study area of this paper (Coronato et al., 1999). The related glacio-eustatic-, glacio-isostatic-, and neotectonic-induced relative sea level oscillations left a well-defined mark on coastal landscapes.

This article aims to describe the geomorphology of the Argentine northeastern tip of IGTdf (see Main Map). The mapped area spans 680 km<sup>2</sup>, a region bounded by the Magellan Strait and the Atlantic Ocean to the north and east, the Argentina–Chile international border to the west, and the Bahía Inútil–Bahía San Sebastián (BI-BSSb) depression to the south. A free, open access, vector geomorphological map of

this zone is provided with the hope that it will be a useful tool for multidisciplinary researchers and decision-makers.

## 2. Natural and socio-economic setting

The mapped area is divided in four topographic domains (TDs; Figure 1): To the north, there is an elevated plain (TD 1, 80 m a.s.l. average elevation). The central sector features a wide, low-elevation alluvial plain (Cullen River; TD 2, 20 m a.s.l. average elevation). Pockmarked hills proceed to the south (TD 3, 60 m a.s.l. average elevation), and the San Sebastián Bay depression is located at the southern margin (TD 4). Elevations range from 160 m a.s.l. in the western hills to sea level along the coastal cliffs and the bay, following a gentle slope (Figure 1).

The climate is sub-humid, cold/temperate with a negative hydrological balance most of the year, except in the snowstorms season in winter. Mean annual precipitation is 324.6 mm and mean annual temperature is 5.5°C (Villarreal & Coronato, 2017). Wind blows persistently throughout the year, mainly from the NW, W, and SW; the mean velocity is 23.7 km/h, reaching up to 152 km/h in gusts (Villarreal & Coronato, 2017). These environmental conditions lead to a semiarid steppe ecosystem featuring xerophyte shrubs and grassland vegetation (Cabrera, 1971; Coronato et al., 2008; Roig, 1998).

**CONTACT** Luis Díaz Balocchi ✉ [luis.diazbalocchi@gmail.com](mailto:luis.diazbalocchi@gmail.com) 📍 Centro Austral de Investigaciones Científicas (CADIC), Bernardo Houssay 200, Ushuaia, Tierra del Fuego, Antártida e Islas del Atlántico Sur, Argentina.

📄 Supplemental data for this article can be accessed <https://doi.org/10.1080/17445647.2020.1780168>

© 2020 The Author(s). Published by Informa UK Limited, trading as Taylor & Francis Group on behalf of Journal of Maps

This is an Open Access article distributed under the terms of the Creative Commons Attribution-NonCommercial License (<http://creativecommons.org/licenses/by-nc/4.0/>), which permits unrestricted non-commercial use, distribution, and reproduction in any medium, provided the original work is properly cited.

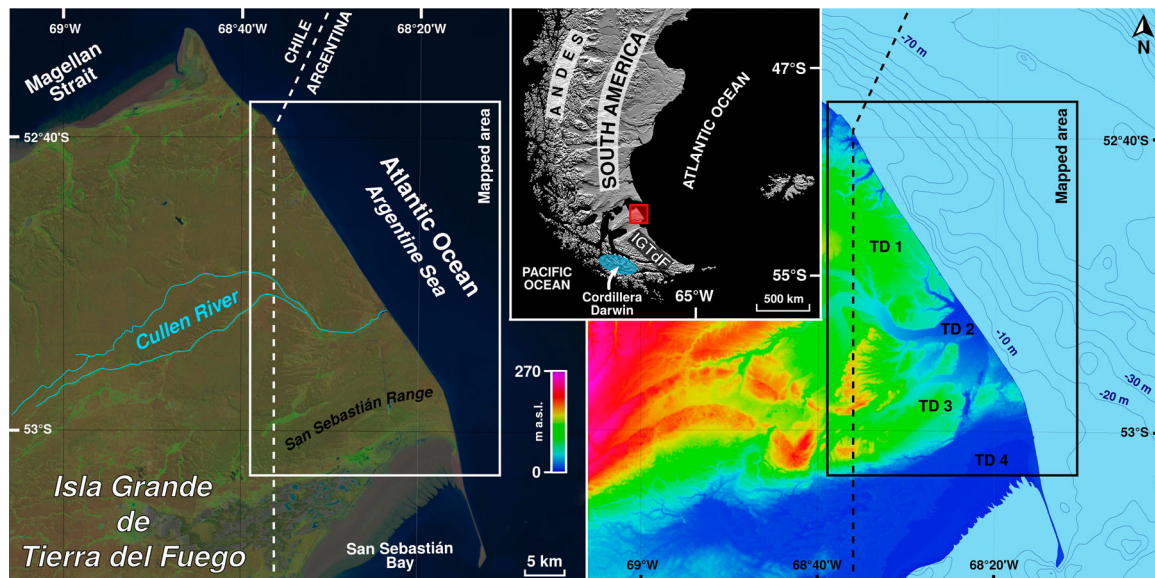


**Figure 1.** Location of the mapped area over a Landsat-8 true color satellite image (left) and an ALOS-PALSAR DEM HSV shaded map (right). Topographic domains (TDs) and main geographical features are indicated.

The Cullen River is the only perennial stream of the study area. Its headwaters are in Chile, about 30 km west of the international boundary, and it discharges into the Atlantic Ocean. Smaller ephemeral and intermittent streams flow along canyons.

The main economic activities in the mapped area are hydrocarbon extraction and sheep breeding. The population is scarce (less than 1000 people) and transient, essentially composed of the workers of oil plants and Cullen Ranch. The nearest city is Río Grande, located 100 km to the southeast.

### 3. Landscape evolution through the Late Cenozoic

During the Neogene, the mapped area was affected by strike-slip deformation and northwards continental drift. The array of the major tectonic troughs followed a SW-NE trend (Diraison et al., 1997, 2000; Ghiglione et al., 2013).

Glacial cycles have occurred in southern South America since the Late Miocene (Mercer & Sutter, 1982; Wenzens, 2006). Glaciations affected northern IGTdF as lobe glaciers fed by the ice sheets located at the southwestern part of the island. These lobes expanded northeastwards, along the tectonic depressions, occupying the piedmont plains and reaching the present-day Atlantic coast (Figure 2) (Auer, 1956; Caldenius, 1932; Feruglio, 1950; Nordenskjöld, 1899). The morainic ridges and belts related to the oldest glaciations registered on IGTdF are recognized around the Magellan Strait and the BI-BSSb depression (Bentley et al., 2005; Clapperton et al., 1995; Coronato et al., 2004; Darvill et al., 2014, 2015, 2017; Glasser & Jansson, 2008; Meglioli, 1992; Rabassa et al., 2011; Rutter et al., 2012) (Figure 2).

Meglioli (1992) recognized three glacial stratigraphic units in this study area and named them ‘Pampa de Beta’, ‘Río Cullen’, and ‘Sierras de San Sebastián’, that would correspond with the Great Patagonian Glaciation (GPG, ca. 1.1 Ma BP; Mercer, 1976), Post-GPG 1 (<1 Ma BP to >760 ka BP; Coronato et al., 2004), and Post-GPG 2 (<760 ka BP to >315 ka BP; Coronato et al., 2004), respectively. Darvill et al. (2015) proposed a much younger chronology based on cosmogenic nuclide dating of associated outwash sediments. The ages of the Río Cullen and Sierras de San Sebastián glaciation would be ca. 45.6 ka BP and ca. 30.1 ka BP, respectively. Griffing (2018) carried out magnetostratigraphic studies on glacial sediments, obtaining a chronology that coincides with Meglioli’s (1992) proposal.

Fluvial processes have oscillated during the Late Cenozoic, controlled mainly by climatic and relative sea level changes. Base level changes have caused incision, stream capture, and terrace development (Codignotto & Malumián, 1981).

Relative sea level changes have induced marine transgressions and regressions that are evidenced as fossil marshes, raised shorelines and beach ridges, marine terraces, incised canyons, and cliffs (Bujalesky, 2007; Codignotto & Malumián, 1981; De Muro et al., 2015, 2017, 2018; Isla et al., 1991; Vilas et al., 1999; among others).

The eastern coast of southern South America is considered a stable passive margin (Schellmann & Radtke, 2010). Nevertheless, purely eustatic sea level oscillations could be ruled out due to the neotectonic activity at both the Magellan Strait (Bentley & McCulloch, 2005; De Muro et al., 2017, 2018) and the eastern coast of Patagonia (Rostami et al., 2000). Deglaciation would have not only produced sea level rise through

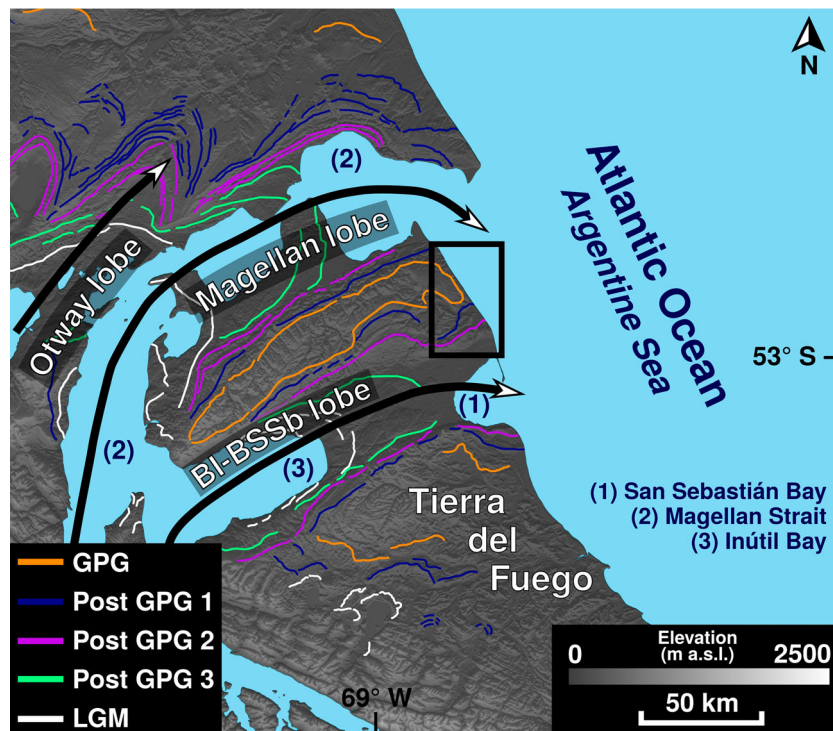


**Figure 2.** Map of ice lobe limits over southern Patagonia and Tierra del Fuego for the Great Patagonian Glaciation (GPG), Post-GPG 1, 2, and 3, and the Last Glacial Maximum (LGM) (based on Rabassa et al., 2011). The base layer is a GMTED2010 DEM.

glacio-eustasy, but also land uplift caused by post-glacial isostatic adjustment (Rostami et al., 2000; Schellmann & Radtke, 2010).

The San Sebastián Bay formed in a tectonic depression deepened by glacial erosion that was flooded during the Middle Holocene (Bujalesky, 2007). Since then, relative sea level has dropped and coastal progradation developed around the bay margins (Vilas et al., 1999).

The present-day macromareal tides (~11 m) and rough waters cause coastal erosion, while southwards longshore drift has created El Páramo spit (Bujalesky, 2007).

Strong winds trigger deflation, generating scattered blowouts that coat significant areas of the landscape. A combination of aeolian-lacustrine processes produced shallow lakes and pans (Arche & Vilas, 2001; Codignotto & Malumián, 1981; Isla et al., 1991; Vilas et al., 1999; Villarreal & Coronato, 2017).

#### 4. Previous research and mapping

Nordenskjöld (1899), Caldenius (1932) and Feruglio (1950) made the first regional approach to an ice limits map for southern South America. Meglioli (1992) proposed a glacial stratigraphic model for the Bahía Inútil-Bahía San Sebastián and Magellan Strait lobes based on field observations, mapping, and sample dating. His map was later adjusted by Rabassa et al. (2000, 2011), Coronato et al. (2004), Glasser and Jansson (2008), Coronato and Rabassa (2011), Rutter et al. (2012), and Darvill et al. (2014, 2017). Olivero et al. (2007)

supplied the first geological map covering all of IGTdF. Codignotto and Malumián (1981) outlined a geological map of the here studied area.

Coastal morphology was first described by Codignotto (1975, 1979) and later revised by Bujalesky (1990, 2007), Isla et al. (1991), and Vilas et al. (1999). Isla and Schnack (1995) and Mouzo (2005) mapped submarine features. Arche and Vilas (2001) and Villarreal and Coronato (2017) examined aeolian landforms located in the bay environment.

#### 5. Methods

The maps of Codignotto and Malumián (1981), Isla et al. (1991), Meglioli (1992), Olivero et al. (2007), and Darvill et al. (2014) provided a basis for the map presented here.

The mapping process employed Landsat-8 panchromatic band (15 m spatial resolution) and Sentinel-2 visible spectrum bands (10 m spatial resolution) satellite images mounted on a GIS project on QGIS 2.16. An ALOS-PALSAR (12.5 m horizontal spatial resolution) DEM was used as a topographic base. The survey was complemented by detailed validation using high-resolution images from Google Earth™ and Bing Maps™ displayed by the QGIS OpenLayers plugin. All features were manually mapped at a 1:20,000 scale (or finer) to obtain smoother outlines. The polygons of geomorphological units were represented using 70% opacity and the gullies were shaded gray with 10% opacity. The base layer is a hillshade map derived from ALOS-PALSAR data. Elevation points were placed in several



positions to aid topography visualization. Bathymetric contours (10 m equidistance) obtained from GEBCO 2019 data were plotted over the sea.

The resulting SVG file was edited and exported as a PDF file in Inkscape 0.91. The map is projected in UTM Zone 19S using a WGS 84 datum. It is designed to be printed on A1 size paper at a scale of 1:60,000. Landforms were revised in the field to verify remote interpretation and to improve descriptions and illustrations. These illustrations are shown as figures in this manuscript and in the online supplemental material.

## 6. Landform description

### 6.1. Glacial and periglacial landforms

#### 6.1.1. Hummocky moraines

These landforms appear in the southern sector of the map in two subparallel belts. This unit shows a pock-marked topography with mounds and holes that average 50 m in diameter and 4 m in depth (Figure 3). These landforms have been assigned a glacial origin and classified as kame and kettle topography or hummocky moraines (Darvill et al., 2014, 2017; Díaz Balocchi et al., 2018a; Meglioli, 1992).

The southernmost hummocky moraine belt (78.5 km<sup>2</sup>) is a 3 km wide elevated area (30 m over the surrounding relief). It extends SW-NE for 25 km in a smooth curve. It is assigned to the Sierras de San Sebastián glaciation (Meglioli, 1992). The other

hummocky moraine belt (33 km<sup>2</sup>) develops about 4 km to the north and is parallel to the former belt. It is 18 km in length and its width varies from 2.5 km in the west to 0.5 km in the east, where it narrows before reaching the coast. It rises about 20 m over the surrounding relief. This belt is related to the Río Cullen glaciation (Meglioli, 1992). Towards the coast, this moraine is found at a lower level than at inland and its shape is distorted, possibly due to reworking by meltwater coming from the southern belt thaw.

#### 6.1.2. Overridden moraine

In the inner part of the moraine belts, occupying a lower topographic level, there is a flat, or residual hummocky, landscape (Figure 4). These areas usually show a convex topographic profile and exhibit some inherited subdued landforms like hummocks and minor depressions filled with sediments. This unit is assumed to be an older hummocky moraine overridden by later ice advances. In the northern shore of San Sebastián Bay these moraines are further reworked, probably by aeolian processes and marine ingressions that reached up to 25 m over the present-day sea level during the Middle Pleistocene (Bujalesky, 2007).

#### 6.1.3. Till plain

North of the Cullen River floodplain, there is a relatively horizontal relief formed by a till cover. It extends over the northern part of the map and is only disrupted by gully incisions (Figure 5). The surface of this plain is

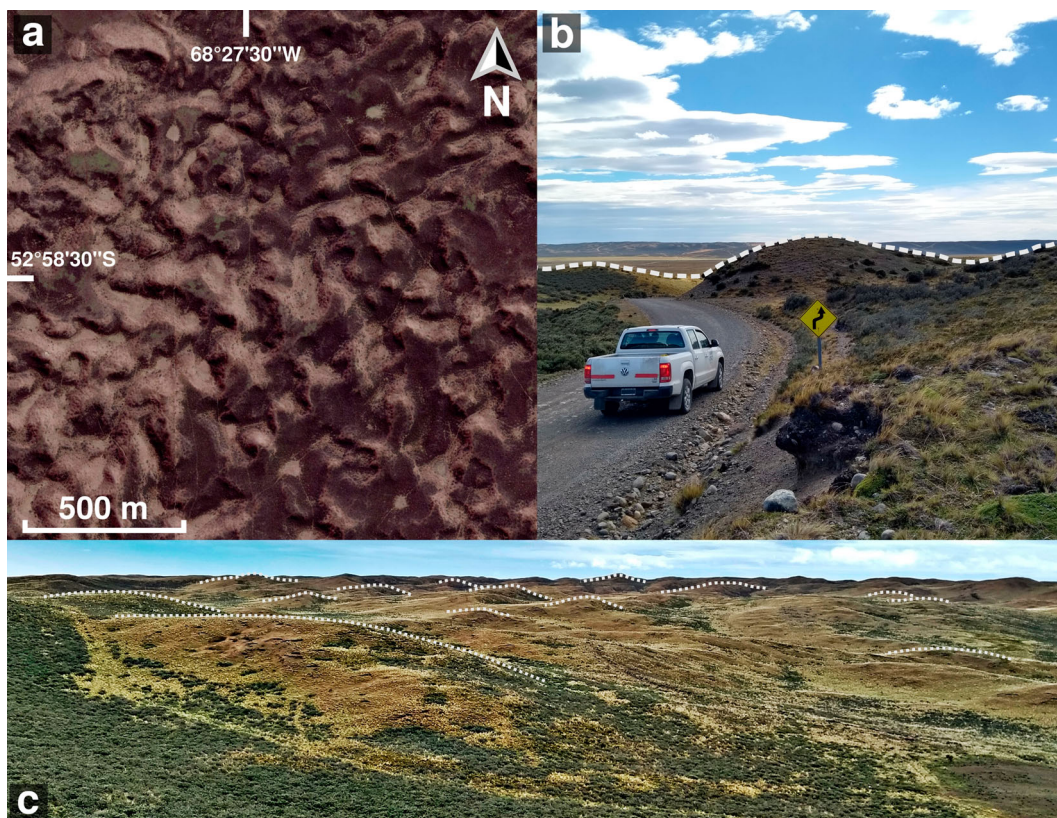


**Figure 3.** Hummocky moraine aspect. Google Earth™ satellite image (a). Appearance of hummocks in the field (b and c).



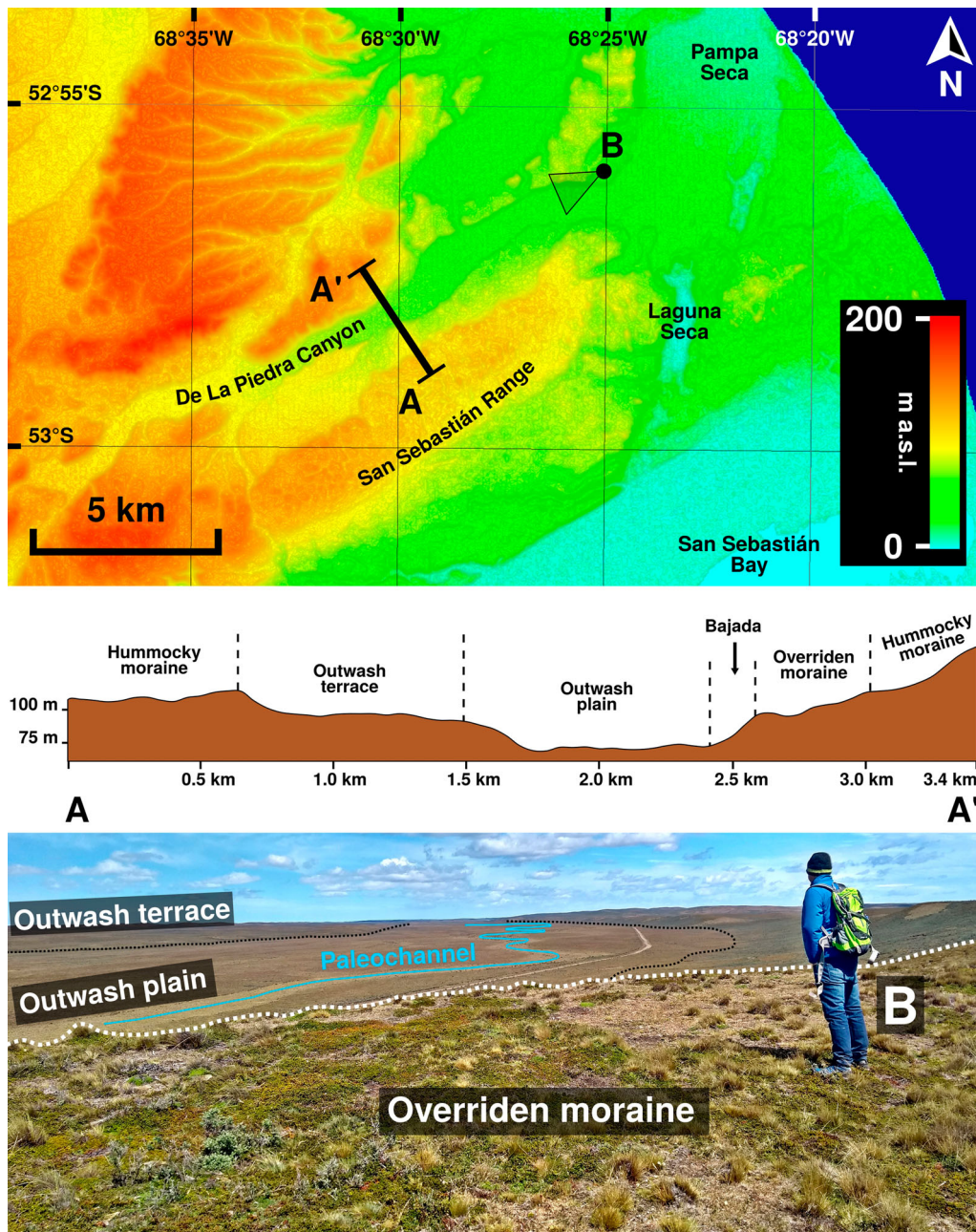


**Figure 4.** De La Piedra Canyon. Location of the topographic profile and photo over an ALOS-PALSAR DEM HSV shaded map (top). Topographic profile (middle). Field picture of the outwash plain showing a well preserved sinuous paleochannel surrounded by an outwash terrace to the south and an overridden moraine level to the north (bottom).

214 km<sup>2</sup>, and it is elevated 80 m a.s.l. on average, with a smooth slope (<1°) dipping eastwards. The deposits related to this landform show intercalated strata of till and clast-supported gravels (Díaz Balocchi et al., 2018b) and are linked to the Pampa de Beta glaciation (Díaz Balocchi et al., 2018b; Meglioli, 1992).

#### 6.1.4. Dissected glacial tableland

There is a sector of singular topography around Pirámide Canyon. Over a subhorizontal tableland (52 km<sup>2</sup>) elevated 150 m a.s.l. (and about 25 m over surrounding relief) with a slope of 0.5° dipping eastwards, there is a dense gullies network that shows a subparallel to dendritic pattern with a W-E orientation. The flat surface exhibits coarse sand and gravel with

dispersed boulders (up to 1 m in diameter). Outcrops display glacial gravels and diamicts that discordantly cover Neogene rocks. A small part of this unit appears northwards, across the Cullen River floodplain, and is surrounded by the Till plain unit. Considering the appearance, degree of consolidation of its sediments, cross-cutting relationships and elevation, this unit could represent the first pre-GPG glacial surface recognized in Tierra del Fuego, corroborating the 'Río Grande glaciation' proposed by Meglioli (1992).

#### 6.1.5. Ice-marginal erosive ridges

The southwestern study area shows a topography dominated by elongated hills that follow a W-E orientation. This unit (12 km<sup>2</sup>) is distinguished by narrow

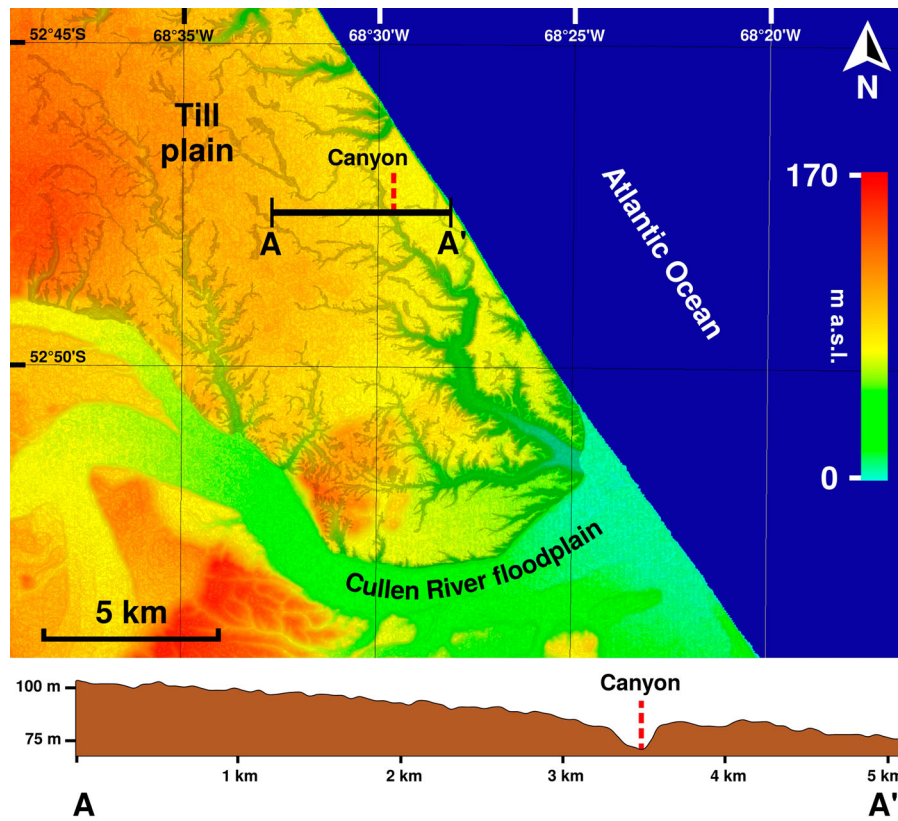


**Figure 5.** Till plain. Location of the topographic profile over an ALOS-PALSAR DEM HSV shaded map (top). Topographic profile (bottom) showing a smooth slope dipping eastwards, only interrupted by a canyon.

(50–80 m wide) and long (up to 900 m) elevations ( $\sim 5$  m) recognized as straight to undulated ridges in aerial photos (Figure 6). These landforms were sculpted in Neogene sandstones by subglacial and ice-marginal erosive processes, possibly related to the Sierras de San Sebastián glaciation, and could be considered bed-rock drumlins. In several locations a thin till cover coats the ridges (Figure 6).

#### 6.1.6. Moraine collapse and subsidence features (depressed hummocky moraine, closed and pitted outwash basins)

Inside the moraine belts, there are several depressed areas. These features appear as elongated basins of smoothed topography that are clearly lower than the surrounding moraine. Over the surface they keep the original hummocky relief or are covered by pitted outwash or lacustrine sediments. Nowadays these depressions can be connected to the drainage network through longitudinal channels or develop closed drainage basins, as in the case of Laguna Salada. These landforms are interpreted as remains of hummocky moraines that were affected by subsidence due to the melting, faulting, and slumping of ice-rich cores of till, or simply due to the thawing of large isolated ice blocks.

#### 6.1.7. Outwash plains and terraces

Between both hummocky moraine belts there are flat topography areas formed by glacial outwash sediments.

They are smooth, featureless surfaces of sand and gravel that gently grade away from former ice limits (Darvill et al., 2014) where poorly preserved braided and meandering paleochannels are recognized. These outwash levels were cut by subsequent fluvial erosion, developing terraces and canyons (Figure 4). The southern moraine belt shows a well-defined meltwater channel that was mapped as a different unit.

Outside the plains, two moraine collapse basins are covered by pitted outwash sediments related to high discharge of meltwater. The thawing of isolated ice blocks shaped depressions that at the present are reworked as aeolian blowouts and ephemeral ponds.

#### 6.1.8. Kettle depressions

Northwards of the San Sebastián hummocky moraine belt there are two depressed units ( $3 \text{ km}^2$ ) oriented in a N-S direction, dominated by kettle holes. The cavities reach up to 250 m diameter and 10 m depth. Their bottoms are flat and filled with fine-grained sediments, reworked by aeolian, ephemeral fluvial, and lacustrine processes. The units were differentiated because the northernmost one shows signs of strong erosion by meltwater streams.

#### 6.1.9. Thaw slump

In the center of the map there is a spoon-shaped lowland ( $2.4 \text{ km}^2$ ). This unit is considered a thaw slump limited by a subcircular eroded scarp to the west. In the central



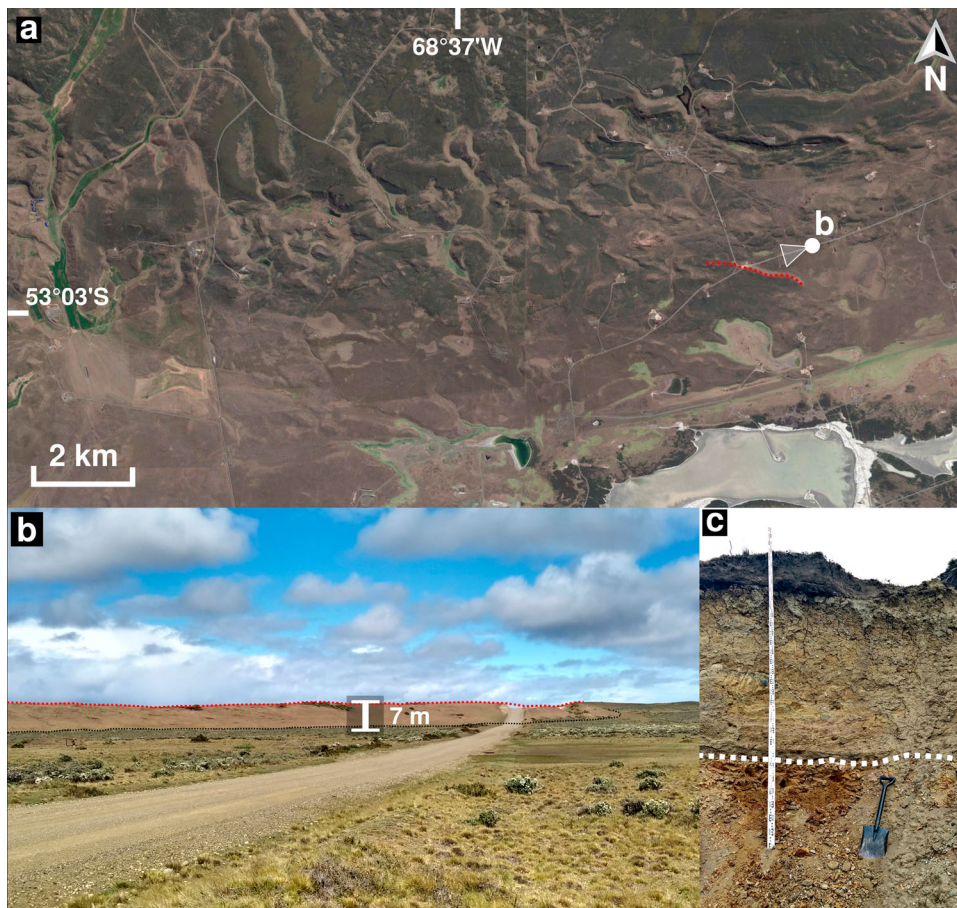


**Figure 6.** Elongated subglacial and ice-marginal erosive hills. Google Earth™ satellite image (a). Field view of the hills (b). Reddish Neogene sedimentary rocks covered by pale brown till following an erosive contact (c).

sector of the unit, there is a fallen area where hummocks are diminished, tilted, and surrounded by ponds. Eastwards of this surface, there is a region of blurred pushed mounds that form the deposits of the toe of the slump.

## 6.2. Fluvial landforms

### 6.2.1. Cullen River channels and floodplain

The Cullen River is found in the central sector of the map. Present-day activity of this fluvial system is restricted to meandering/anastomosing channels and its floodplain (Figure 7). Tidal influenced lagoons and channels controlled by the longshore drift are located around the estuary that develops on the river mouth.

### 6.2.2. Cullen River terraces

At least three terrace levels are visible on the margins of the current Cullen River floodplain. To the west, two unpaired cut terrace levels are found at 75 and 105 m a.s.l. (Figure 7). In the eastern sector, at 20 m a.s.l., there is a terrace molded on outwash deposits.

### 6.2.3. Gullies and canyons

Base level changes have caused the incision of gullies in a great portion of the mapped landscape. The first

group of gullies is located over the dissected glacialic tableland and was described above.

Another group of gullies cut over the Till plain unit, following a SW-NE to NW-SE disposition. They show a subdendritic pattern and highly smoothed slopes (Figure 8a). These landforms are evidence of ancient fluvial regimes of high erosive power, probably related to deglaciation or rapid base level changes. Some of these gullies developed large canyons of up to 60 m depth. They can reach the coastal cliffs as hanging valleys (e.g. Tortuga Canyon) or the sea level in estuaries (e.g. Beta and Alfa canyons) (Figure 8b and c).

### 6.2.4. Minor ephemeral streams

The mapped area presents minor ephemeral streams that follow an arrangement controlled by structural and morphological features (Díaz Balocchi, 2017). These creeks are usually dry but can conduct temporary discharge during floods or in the snowmelt season. In specific locations (e.g. Pirámide Canyon), the phreatic level reaches the surface, forming intermittent ponds and wet meadows.

### 6.2.5. Bajada

Inside the De La Piedra Canyon, several alluvial fans laterally coalesce forming a bajada. This unit covers



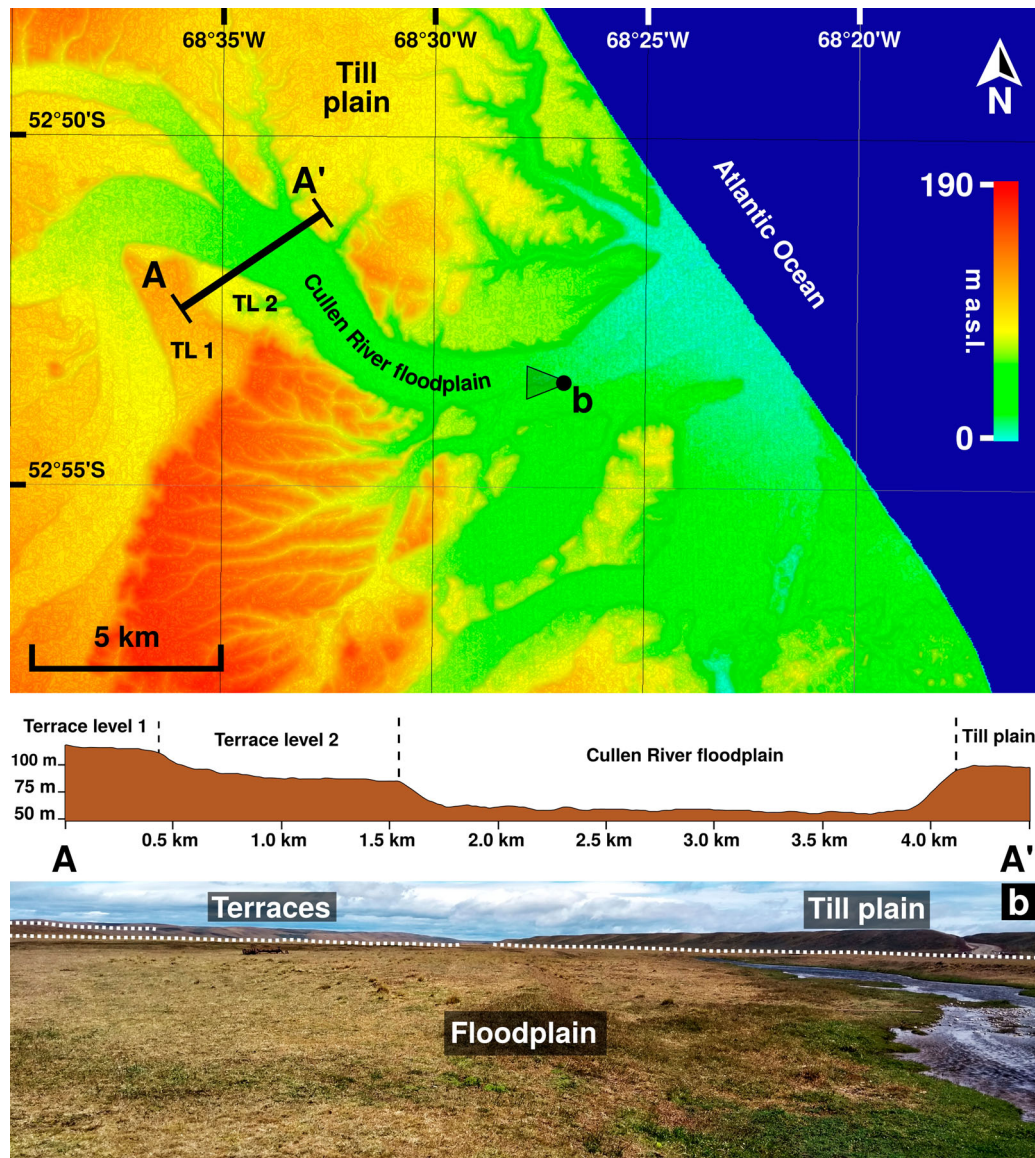


**Figure 7.** Cullen River floodplain and terraces. Location of the topographic profile and field photograph over an ALOS-PALSAR DEM HSV shaded map (top). Topographic profile of terraces (middle). View of the Cullen River floodplain and terraces (bottom).

1.3 km<sup>2</sup> and is made of till reworked by colluvial and alluvial processes.

### 6.3. Coastal landforms

#### 6.3.1. Active cliffs

Active cliffs are found along 40 km in a NNW-SSE orientation, between Espíritu Santo Cape and Nombre Cape. They climb from 10 m up to 90 m height in a northwards direction (Bujalesky, 2007). The cliffs are actively retreating with episodic collapse events triggered by extraordinary storm waves and tides (Bujalesky, 1990, 2007), increased by regular mass-wasting processes over unstable slopes.

#### 6.3.2. Paleocliffs

A paleocliff is recognized in the southern portion of the study area, surrounding San Sebastián Bay (Codignotto & Malumián, 1981). It is about 4 m high and 20 km

long, along a WSW-ENE direction. Another paleocliff (40 m high) was identified immediately northwards, following a SSW-NNE orientation.

#### 6.3.3. Beaches

A series of sandy beaches are positioned in a thin strip between the active cliffs and the coastline in most of the eastern part of the study area. These beaches are affected by macromareal tides and strong waves that develop a southwards longshore drift (Codignotto & Malumián, 1981; Isla et al., 1991). The beaches are wider north of the Cullen River (about 200 m); while in the south they reach a maximum width of 100 m. The beaches surrounding El Páramo Peninsula will be described below.

#### 6.3.4. Estuaries

The river mouths of the Cullen River and the streams at Alfa and Beta canyons are reworked by macromareal



**Figure 8.** Field view of old canyons and gullies cutting the till plain. They show smooth and eroded slopes (a) that can reach the coastline as hanging valleys or at sea level (b and c).

tides and wave action. These small wave-dominated estuaries display barrier beaches, lagoons and inlets controlled by the southwards longshore drift. The Cullen River estuary also presents some tidal channels that are active in flood tides produced by severe storms.

### 6.3.5. Supratidal flat (and marshes)

A supratidal flat surrounds the San Sebastián Bay. This unit is a 3 km-wide, 42 km<sup>2</sup> semicircular belt not influenced by ordinary tides. It features a plain topography with a smooth (<0.1°) slope dipping to the south and east. The sediments composing this unit are fine silt and pore salts highly susceptible to erosion. The main landforms are shallow (<1 m) ponds and lagoons of hydro-aeolian erosion origin (Bujalesky, 2007; Isla et al., 1991; Villarreal & Coronato, 2017).

### 6.3.6. Intertidal flat (muddy/mixed)

Inwards the bay, the action of macromareal tides produced an intertidal flat (34 km<sup>2</sup>) that displays a dendritic to subparallel tidal channel network. These channels have meandering to straight patterns and reach depths of over 3 m and widths of over 50 m (Bujalesky, 2007). The tidal currents transport sediment in a clockwise direction with grain-size increasing southwards due to wave action (Bujalesky, 2007; Isla et al., 1991).

### 6.3.7. Gravel spit

El Páramo Peninsula is a 20 km long gravel spit formed by southwards longshore drift (Codignotto, 1975). Its width oscillates between 200 and 1200 m (Kokot, 2010). The northern sector (sensu Isla et al., 1991) is included in the here presented map. It is composed of gravel beach ridges parallel to the paleocliff in the northernmost part that progressively turn to a N-S orientation as one moves southwards (Bujalesky, 1990). Gravels are the main constituents of the spit, although a sandy matrix is always present (Isla et al., 1991). The Atlantic beach is 100 m wide, while the bay beach is steeper and only 50 m wide (Bujalesky, 1990).

## 6.4. Aeolian and lacustrine landforms

This unit is not differentiated on the map because either: (1) it overlaps other units that have a stronger influence on the landscape, or (2) its small-sized landforms cannot be clearly displayed at the chosen scale.

### 6.4.1. Erosional landforms

They are recognized as blowouts and minor water bodies. Wind activity reworks marsh and supratidal sediments producing muddy lunettes that surround shallow, W-E elongated, ponds (up to 4 km long) (Arche & Vilas, 2001; Villarreal & Coronato, 2017).



Northwards, small blowouts (up to 300 m in diameter) coat most of the surface. Current aeolian and ephemeral lacustrine processes modify preexistent depressions of glacial or aeolian origin.

#### 6.4.2. Isolated climbing dunes

Isolated dunes formed by coarse sand and fine pebbles partially climb along coastal cliffs, at the eastern sector of the study area, mainly between Alfa and Tortuga canyons. These very elongated barchans to linear dunes advance in a NNE-SSW direction, parallel to the coast, and are fed by beach deposits.

#### 6.5. Anthropogenic landforms

Roads and oil well pads are the main human landforms. Some feedlots show denudation and incipient soil erosion caused by sheep. Structures built on oil plants, ranches, and small settlements complete this unit.

### 7. Conclusions

A geomorphological map at a 1:60,000 scale of the northeastern extreme of Isla Grande de Tierra del Fuego, Argentina, was produced. Interpretation of satellite images and field recognition were used to identify glacial, periglacial, fluvial, coastal, aeolian, lacustrine, and anthropogenic landforms. A simplified landscape evolution of the study area during the Late Cenozoic is suggested following these stages:

- (1) Neogene N-S tectonic extension shaped eastwards and northeastwards oriented troughs (e.g. proto-Magellan Strait).
- (2) Structurally controlled drainage developed over the main faults (e.g. proto-Cullen River).
- (3) During the Early Pleistocene (and presumably earlier) piedmont glaciers formed massive glacial tablelands (e.g. Pampa de Beta).
- (4) Deglaciation led to the flow of large, highly erosive rivers. Also, land uplift might have aided the incision of canyons and terraces, as well as the formation of the paleoclimbs.
- (5) The glacial advances of the BI-BSSb ice lobe during the Middle Pleistocene further dug the valley. The Río Cullen and Sierras de San Sebastián moraines indicate the limits of each advance. Ice-marginal erosive features were chiseled over the bedrock in the southern zone.
- (6) Final ice degradation combined with periglacial, fluvial, and mass-wasting processes remodeled previous glacial landforms. Abundant meltwater produced proglacial outwash plains. Multi-causal land uplift restarted the formation of terraces. Aeolian erosion reshaped glacial depressions as blowouts.

- (7) During the Middle Holocene transgression, the San Sebastián Bay was flooded. Southwards long-shore drift shaped El Páramo spit.

### Acknowledgements

We thank Total Austral S.A. for their support with accommodation. Estancia Cullen allowed us to use their private roads. Cristina San Martín, Candela Gorza, Ramiro López and Mauro Gómez Samus helped us during fieldwork. We are very grateful to Matteo Spagnolo, Chris Orton, and Sandro De Muro for their reviews and suggestions. Finally, we thank Dante Francomano and Ryne Flanagan for the revision of English language.

### Disclosure statement

No potential conflict of interest was reported by the author(s).

### Funding

Fieldwork was funded by a PIDUNTDF -B- 05/2016 research project granted to Juan Federico Ponce by UNTDF.

### Software

The map was generated using QGIS 2.16. Final edition and PDF export were performed using Inkscape 0.9.

### ORCID

Luis Díaz Balocchi  <http://orcid.org/0000-0001-8763-7722>

### References

- Arche, A., & Vilas, F. (2001). Sedimentos eólicos de grano fino en la Bahía de San Sebastián, Tierra del Fuego, Argentina. *Journal of Iberian Geology*, 27, 159–173.
- Auer, V. (1956). The Pleistocene of Fuego-Patagonia. Part I: The ice and interglacial ages. *Annales Academiae Scientiarum Fennicae, A, III*, 45, 1–222.
- Bentley, M. J., & McCulloch, R. D. (2005). Impact of neotectonics on the record of glacier and sea level fluctuations, Strait of Magellan, southern Chile. *Geografiska Annaler: Series A, Physical Geography*, 87(2), 393–402. <https://doi.org/10.1111/j.0435-3676.2005.00265.x>
- Bentley, M. J., Sugden, D. E., Hulton, N. R., & McCulloch, R. D. (2005). The landforms and pattern of deglaciation in the Strait of Magellan and Bahía Inútil, southernmost South America. *Geografiska Annaler: Series A, Physical Geography*, 87(2), 313–333. <https://doi.org/10.1111/j.0435-3676.2005.00261.x>
- Bujalesky, G. G. (1990). *Morfología y dinámica de la sedimentación costera en la península El Páramo, Bahía San Sebastián, Isla Grande de la Tierra del Fuego* [Unpublished doctoral dissertation]. Facultad de Ciencias Naturales y Museo, Universidad Nacional de La Plata.
- Bujalesky, G. G. (2007). Coastal geomorphology and evolution of Tierra del Fuego (Southern Argentina). *Geologica Acta*, 5(4), 337–362. <https://doi.org/10.1344/105.000000294>

- Cabrera, A. L. (1971). Fitogeografía de la República Argentina. *Boletín de la Sociedad Argentina de Botánica*, 14, 1–42.
- Caldenius, C. (1932). Las Glaciaciones Cuaternarias en la Patagonia y Tierra del Fuego. *Geografiska Annaler*, 14, 1–164. <https://doi.org/10.1080/20014422.1932.11880545>
- Clapperton, C. M., Sugden, D. E., Kaufman, D. S., & McCulloch, R. D. (1995). The last glaciation in central Magellan Strait, southernmost Chile. *Quaternary Research*, 44(2), 133–148. <https://doi.org/10.1006/qres.1995.1058>
- Codignotto, J. O. (1975). *Geología y Rasgos Geomorfológicos de la Patagonia Austral Extraandina, entre el río Chico de Gallegos (Santa Cruz) y la bahía de San Sebastián (Tierra del Fuego)* [Unpublished doctoral dissertation]. Facultad de Ciencias Exactas y Naturales, Universidad de Buenos Aires.
- Codignotto, J. O. (1979). *Hojas Geológicas 63a Cullen, 64a Bahía San Sebastián y 65b Río Grande*. Servicio Geológico Nacional.
- Codignotto, J. O., & Malumíán, N. (1981). Geología de la región al norte del paralelo 54 S de la Isla Grande de Tierra del Fuego. *Revista de la Asociación Geológica Argentina*, 36(1), 44–88.
- Coronato, A., Coronato, F., Mazzoni, E., & Vázquez, M. (2008). The physical geography of Patagonia and Tierra del Fuego. In J. Rabassa (Ed.), *The Late Cenozoic of Patagonia and Tierra del Fuego* (pp. 13–55). Elsevier. [https://doi.org/10.1016/S1571-0866\(07\)10003-8](https://doi.org/10.1016/S1571-0866(07)10003-8)
- Coronato, A., Meglioli, A., & Rabassa, J. (2004). Glaciations in the Magellan Straits and Tierra del Fuego, southernmost South America. In J. Ehlers & P. L. Gibbard (Eds.), *Quaternary glaciations extent and chronology part III: South America, Asia, Africa, Australasia, Antarctica* (pp. 45–48). Elsevier. [https://doi.org/10.1016/S1571-0866\(04\)80110-6](https://doi.org/10.1016/S1571-0866(04)80110-6)
- Coronato, A., & Rabassa, J. (2011). Pleistocene glaciations in Southern Patagonia and Tierra del Fuego. In J. Ehlers, P. L. Gibbard, & P. D. Hughes (Eds.), *Quaternary glaciations – extent and chronology: A closer look* (pp. 715–727). Elsevier. <https://doi.org/10.1016/B978-0-444-53447-7.00051-9>
- Coronato, A., Salemme, M., & Rabassa, J. (1999). Palaeoenvironmental conditions during the early peopling of southernmost South America (Late Glacial-Early Holocene, 14–8 ka BP). *Quaternary International*, 53–54, 77–92. [https://doi.org/10.1016/S1040-6182\(98\)00009-3](https://doi.org/10.1016/S1040-6182(98)00009-3)
- Darvill, C. M., Bentley, M. J., Stokes, C. R., Hein, A. S., & Rodés, Á. (2015). Extensive MIS 3 glaciation in southernmost Patagonia revealed by cosmogenic nuclide dating of outwash sediments. *Earth and Planetary Science Letters*, 429, 157–169. <https://doi.org/10.1016/j.epsl.2015.07.030>
- Darvill, C. M., Stokes, C. R., Bentley, M. J., Evans, D. J., & Lovell, H. (2017). Dynamics of former ice lobes of the southernmost Patagonian Ice Sheet based on a glacial landsystems approach. *Journal of Quaternary Science*, 32(6), 857–876. <https://doi.org/10.1002/jqs.2890>
- Darvill, C. M., Stokes, C. R., Bentley, M. J., & Lovell, H. (2014). A glacial geomorphological map of the southernmost ice lobes of Patagonia: The Bahía Inútil–San Sebastián, Magellan, Otway, Skyring and Río Gallegos lobes. *Journal of Maps*, 10(3), 500–520. <https://doi.org/10.1080/17445647.2014.890134>
- De Muro, S., Brambati, A., Tecchiato, S., Porta, M., & Ibba, A. (2017). Geomorphology of marine and transitional terraces and raised shorelines between Punta Paulo and Porvenir, Tierra del Fuego, Straits of Magellan – Chile. *Journal of Maps*, 13(2), 311–321. <https://doi.org/10.1080/17445647.2017.1295406>
- De Muro, S., Di Grande, A., Brambati, A., & Ibba, A. (2015). Geomorphology map of the marine and transitional terraces and raised shorelines of the Península Juan Mazía, Tierra Del Fuego. Straits of Magellan – Chile. *Journal of Maps*, 11(5), 698–710. <https://doi.org/10.1080/17445647.2014.970592>
- De Muro, S., Tecchiato, S., Porta, M., Buosi, C., & Ibba, A. (2018). Geomorphology of marine and glacio-lacustrine terraces and raised shorelines in the northern sector of Península Brunswick, Patagonia, Straits of Magellan, Chile. *Journal of Maps*, 14(2), 135–143. <https://doi.org/10.1080/17445647.2018.1441759>
- Díaz Balocchi, L. (2017, August). Implicancias geomorfológicas y estructurales en el control del drenaje superficial al norte de la Bahía San Sebastián, Isla Grande de Tierra del Fuego. In Asociación Geológica Argentina (Ed.), *Proceedings of the 20th Argentine geological congress (symposium 7)* (pp. 38–42). Asociación Geológica Argentina.
- Díaz Balocchi, L., Ponce, J. F., Tripaldi, A., & Magneres, I. (2018a, September). Asociaciones de geoformas y depósitos del sector norte del lóbulo Bahía Inútil – Bahía San Sebastián, Tierra del Fuego. In Bouza, P., Veiga, G., Piovano, E., Zárata, M., & Bilmes, A. (Eds.), *Proceedings of the 7th Argentinian Congress on Quaternary and Geomorphology* (pp. 206–207). Asociación Argentina de Cuaternario y Geomorfología.
- Díaz Balocchi, L., Ponce, J. F., Tripaldi, A., & Magneres, I. (2018b, September). Caracterización geomorfológica y sedimentológica de la planicie glaciogénica del extremo norte del sector argentino de la Isla Grande de Tierra del Fuego. In Bouza, P., Veiga, G., Piovano, E., Zárata, M., & Bilmes, A. (Eds.) *Proceedings of the 7th Argentinian congress on quaternary and geomorphology* (pp. 208–209). Asociación Argentina de Cuaternario y Geomorfología.
- Diraison, M., Cobbold, P. R., Gapais, D., & Rossello, E. A. (1997). Magellan Strait: Part of a Neogene rift system. *Geology*, 25(8), 703–706. [https://doi.org/10.1130/0091-7613\(1997\)025<0703:MSPOAN>2.3.CO;2](https://doi.org/10.1130/0091-7613(1997)025<0703:MSPOAN>2.3.CO;2)
- Diraison, M., Cobbold, P. R., Gapais, D., Rossello, E. A., & Le Corre, C. (2000). Cenozoic crustal thickening, wrenching and rifting in the foothills of the southernmost Andes. *Tectonophysics*, 316(1–2), 91–119. [https://doi.org/10.1016/S0040-1951\(99\)00255-3](https://doi.org/10.1016/S0040-1951(99)00255-3)
- Fernández, M., Ponce, J. F., Zangrando, F. J., Borronei, A. M., Musotto, L. L., Alunni, D., & Vázquez, M. (2018). Relationships between terrestrial animal exploitation, marine hunter-gatherers and palaeoenvironmental conditions during the Middle-Late Holocene in the Beagle Channel region (Tierra del Fuego). *Quaternary International*. Advance online publication. <https://doi.org/10.1016/j.quaint.2018.05.032>
- Feruglio, E. (1950). *Descripción Geológica de la Patagonia: Vol. 3*. Dirección General de Yacimientos Petrolíferos Fiscales.
- Ghiglione, M. C., Navarrete-Rodríguez, A. T., González Guillot, M., & Bujalesky, G. (2013). The opening of the Magellan Strait and its geodynamic implications. *Terra Nova*, 25(1), 13–20. <https://doi.org/10.1111/j.1365-3121.2012.01090.x>
- Glasser, N., & Jansson, K. (2008). The glacial map of Southern South America. *Journal of Maps*, 4(1), 175–196. <https://doi.org/10.4113/jom.2008.1020>
- Griffing, C. Y. (2018). *Late Cenozoic glaciations and environments in southernmost Patagonia* [Doctoral dissertation].



- Simon Fraser University. <https://summit.sfu.ca/item/17942>
- Isla, F. I., & Schnack, E. (1995). Submerged moraines offshore northern Tierra del Fuego, Argentina. *Quaternary of South America and Antarctic Peninsula*, 9, 205–222.
- Isla, F. I., Vilas, F. E., Bujalesky, G. G., Ferrero, M., Bonorino, G. G., & Miralles, A. A. (1991). Gravel drift and wind effects on the macrotidal San Sebastian Bay, Tierra del Fuego, Argentina. *Marine Geology*, 97(1-2), 211–224. [https://doi.org/10.1016/0025-3227\(91\)90027-2](https://doi.org/10.1016/0025-3227(91)90027-2)
- Kokot, R. R. (2010). Espigas indicadoras de proveniencia de olas en la costa Argentina. *Revista de la Asociación Geológica Argentina*, 67(1), 19–26.
- Meglioli, A. (1992). *Glacial geology and chronology of southernmost Patagonia and Tierra del Fuego* [Unpublished doctoral dissertation]. Lehigh University.
- Mercer, J. H. (1976). Glacial history of southernmost South America. *Quaternary Research*, 6(2), 125–166. [https://doi.org/10.1016/0033-5894\(76\)90047-8](https://doi.org/10.1016/0033-5894(76)90047-8)
- Mercer, J. H., & Sutter, J. F. (1982). Late miocene—earliest pliocene glaciation in southern Argentina: Implications for global ice-sheet history. *Palaeogeography, Palaeoclimatology, Palaeoecology*, 38(3-4), 185–206. [https://doi.org/10.1016/0031-0182\(82\)90003-7](https://doi.org/10.1016/0031-0182(82)90003-7)
- Mouzo, F. (2005). Límites de las glaciaciones Plio-Pleistocenas en la plataforma continental al noreste de la Tierra del Fuego. In Asociación Geológica Argentina (Ed.), *Proceedings of the 16th Argentine Geological Congress* (pp. 787–792). Asociación Geológica Argentina.
- Nordenskjöld, O. (1899). *Geologie, geographie und anthropologie. Swedischen Expedition nach den Magellansländern*. Norstedt and Soner.
- Olivero, E. B., Malumián, N., & Martinioni, D. R. (2007). *Mapa Geológico de la Isla Grande de Tierra del Fuego e Isla de los Estados a escala 1:400.000*. Servicio Geológico Minero Argentino (SEGEMAR).
- Rabassa, J., Coronato, A., Bujalesky, G., Salemme, M., Roig, C., Meglioli, A., Heusser, C., Gordillo, S., Roig, F., Borrromei, A., & Quattrocchio, M. (2000). Quaternary of Tierra del Fuego, southernmost South America: An updated review. *Quaternary International*, 68-71, 217–240. [https://doi.org/10.1016/S1040-6182\(00\)00046-X](https://doi.org/10.1016/S1040-6182(00)00046-X)
- Rabassa, J., Coronato, A., & Martinez, O. (2011). Late Cenozoic glaciations in Patagonia and Tierra del Fuego: An updated review. *Biological Journal of the Linnean Society*, 103(2), 316–335. <https://doi.org/10.1111/j.1095-8312.2011.01681.x>
- Roig, F. (1998). La Vegetación de la Patagonia. In M. N. Correa (Ed.), *Flora Patagónica* (Vol. 8, pp. 48–174). INTA.
- Rostami, K., Peltier, W. R., & Mangini, A. (2000). Quaternary marine terraces, sea-level changes and uplift history of Patagonia, Argentina: Comparisons with predictions of the ICE-4G (VM2) model of the global process of glacial isostatic adjustment. *Quaternary Science Reviews*, 19(14-15), 1495–1525. [https://doi.org/10.1016/S0277-3791\(00\)00075-5](https://doi.org/10.1016/S0277-3791(00)00075-5)
- Rutter, N., Coronato, A., Helmens, K., Rabassa, J., & Zárata, M. (2012). The glacial and loess record of Southern South America. In N. Rutter, A. Coronato, K. Helmens, J. Rabassa, & M. Zárata (Eds.), *Glaciations in North and South America from the Miocene to the last glacial maximum* (pp. 1–23). Springer. [https://doi.org/10.1007/978-94-007-4399-1\\_1](https://doi.org/10.1007/978-94-007-4399-1_1)
- Schellmann, G., & Radtke, U. (2010). Timing and magnitude of Holocene sea-level changes along the middle and south Patagonian Atlantic coast derived from beach ridge systems, littoral terraces and valley-mouth terraces. *Earth-Science Reviews*, 103(1-2), 1–30. <https://doi.org/10.1016/j.earscirev.2010.06.003>
- Vilas, F., Arche, A., Ferrero, M., & Isla, F. (1999). Subantarctic macrotidal flats, cheniers and beaches in San Sebastián Bay, Tierra del Fuego, Argentina. *Marine Geology*, 160(3-4), 301–326. [https://doi.org/10.1016/S0025-3227\(99\)00021-3](https://doi.org/10.1016/S0025-3227(99)00021-3)
- Villarreal, M. L., & Coronato, A. (2017). Characteristics and nature of pans in the semi-arid temperate/cold steppe of Tierra del Fuego. In J. Rabassa (Ed.), *Advances in geomorphology and quaternary studies in Argentina* (pp. 203–224). Springer. [https://doi.org/10.1007/978-3-319-54371-0\\_8](https://doi.org/10.1007/978-3-319-54371-0_8)
- Wenzens, G. (2006). Terminal moraines, outwash plains, and lake terraces in the vicinity of Lago Cardiel (49°S; Patagonia, Argentina)—evidence for Miocene Andean foreland glaciations. *Arctic, Antarctic, and Alpine Research*, 38(2), 276–291. [https://doi.org/10.1657/1523-0430\(2006\)38\[276:TMOPAL\]2.0.CO;2](https://doi.org/10.1657/1523-0430(2006)38[276:TMOPAL]2.0.CO;2)